Purdue University
Purdue e-Pubs

International Refrigeration and Air Conditioning Conference

School of Mechanical Engineering

2010

COP-Based Performance Evaluation of Domestic Refrigerators using Accelerated Flow Evaporators

Jader Barbosa
Federal University of Santa Catarina

Christian Hermes
Federal University of Parana

Paulo Waltrich
Federal University of Santa Catarina

Follow this and additional works at: http://docs.lib.purdue.edu/iracc

Barbosa, Jader; Hermes, Christian; and Waltrich, Paulo, "COP-Based Performance Evaluation of Domestic Refrigerators using Accelerated Flow Evaporators" (2010). *International Refrigeration and Air Conditioning Conference.* Paper 1084.
http://docs.lib.purdue.edu/iracc/1084

This document has been made available through Purdue e-Pubs, a service of the Purdue University Libraries. Please contact epubs@purdue.edu for additional information.
Complete proceedings may be acquired in print and on CD-ROM directly from the Ray W. Herrick Laboratories at https://engineering.purdue.edu/Herrick/Events/orderlit.html

COP-Based Performance Evaluation of Domestic Refrigerators using Accelerated Flow Evaporators

Paulo J. WALTRICH [1], Jader R. BARBOSA Jr. [1*], Christian J. L. HERMES [2]

[1] Department of Mechanical Engineering, Federal University of Santa Catarina, 88040-970, Florianópolis, SC, BRAZIL

[2] Department of Mechanical Engineering, Federal University of Paraná, P.O. Box 19011, 81531-990, Curitiba, PR, BRAZIL

[*] Corresponding Author, Phone: ++55 48 3234 5691, e-mail: jrb@polo.ufsc.br

ABSTRACT

This paper investigates the impact of an alternative evaporator design, the so-called Accelerated Flow Evaporator (AFE), on the performance of household refrigerators. In this novel evaporator concept, the air-side cross section area decreases with the distance from the air flow inlet, accelerating the air as it flows across the tubes and hence improving the air-side local heat transfer coefficient. An AFE heat transfer and pressure drop calculation method proposed elsewhere (Waltrich *et al.*, 2008) has been incorporated into an overall system model (Hermes *et al.*, 2009) to assess the impact of the evaporator geometry on the system *COP*. The results were compared with experimental data obtained in a top-mount refrigerator. The predictions of working pressures, power consumption, cooling capacity and *COP* agreed with the experimental data to within ±10% error bands. The model was subsequently used in an optimization exercise of the AFE geometry that considered both the system *COP* and the evaporator cost.

1. INTRODUCTION

In 'no-frost' refrigerators, compartment cooling relies on forced convection heat transfer between the internal air (assisted by a fan) and a tube-fin evaporator. Since the evaporator is responsible for providing the system cooling capacity, improving its performance is potentially significant as a means of improving the performance of the whole system and, consequently, of promoting material cost savings. The heat exchangers employed as evaporators in 'no-frost' appliances have a number of particular geometric features that hinder the use in rating and design of general heat transfer and pressure drop correlations for tube-fin geometries (Barbosa *et al.*, 2009). Therefore, a number of specific correlations for the Colburn *j*-factor and for the friction factor have been proposed over the years specifically for 'no-frost' evaporators (Karatas *et al*. 1996; Lee *et al.*, 2002; Melo *et al.*, 2006; Barbosa *et al.*, 2009).

The AFE (Cur and Anselmino, 1992) is a special type of 'no-frost' evaporator in which the air-side heat transfer coefficient is locally enhanced as a result of a progressive reduction of the air-side cross-sectional area. While the main advantage of the AFE concept is a reduction of the volume of aluminum in the evaporator, the main drawback is that the flow acceleration increases the air-side pressure drop, thus demanding more pumping power. Waltrich *et al.* (2008) investigated experimentally the thermal-hydraulic performance of AFEs for air flow rates ranging from 30 to 100 m^3/h, under 'dry' conditions (i.e., no condensate or frost formation). Other independent variables were the ratio of the outlet and inlet cross-section area (see Fig. 1) and the fin density. A calculation method for the air-side heat transfer and pressure drop was proposed, which agreed with the experiments to within ±10% for all heat transfer data and ±15% for the majority of the pressure drop data.

The purpose of this paper is to assess the AFE geometric configuration which is capable of providing the highest thermal performance per unit mass of the evaporator. In principle, this can be carried out based on either evaporator ranking criteria (e.g., *j/f* ratio) or, in a more general way, on the component impact on the system *COP* (Pira *et al.*, 2000). In this work, performance evaluation criteria (*PEC*) that account not only for the component impact on the system *COP*, but also for the amount of material (aluminum), are introduced. These are proposed and used in

conjunction with an overall system simulator to find the AFE geometry that optimizes the refrigerator performance, taking the cost of the evaporator into account.

2. SYSTEM MODELING

The model used here is based on the work of Hermes *et al.* (2009), in which the refrigerator was divided into two sub-domains, namely the refrigeration loop (compressor, condenser, capillary tube suction line heat exchanger, and evaporator), as seen in Fig. 2, and the refrigerated compartments (i.e., air flow through the evaporator, frozen- and fresh-food compartments), as seen in Fig. 3.

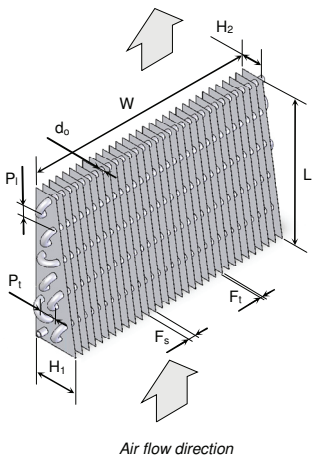

Figure 1. Accelerated flow evaporator.

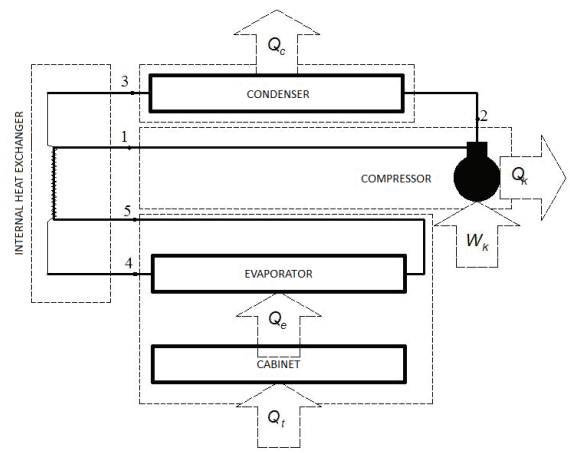

Figure 2. Schematic diagram of the refrigeration loop.

2.1 Refrigeration loop

The refrigerant enthalpy at points 2 to 5 (see Fig. 2) are obtained via energy balances in the compressor, condenser, concentric capillary tube suction line heat exchanger and evaporator, respectively. The heat transfer rates needed in the evaporator and condenser energy balances are obtained from overall thermal conductances calculated according to Waltrich *et al.* (2008) and Melo and Hermes (2009), where the latter is an empirical correlation for natural draft wire-and-tube condensers. The compressor mass flow rate and power are obtained from,

$$m = \left[a + b\left(\left(p_c / p_e\right)^{c_v/c_p} - 1\right)\right] v_1^{-1} \tag{1}$$

$$W_k = c + d \cdot m\left(h_{2,s} - h_1\right) \tag{2}$$

where a, b, c and d are fitted empirically using compressor data obtained from the manufacturer's catalog (Waltrich, 2008). The heat transfer from the compressor shell to the surroundings is given by,

$$Q_k = UA_k\left(T_2 - T_a\right) \tag{3}$$

where the thermal conductance UA_k is assumed constant (≅ 2 W/K). The temperature of the refrigerant entering the compressor is calculated based on the definition of the effectiveness of the suction line heat exchanger given by,

$$T_1 = T_5 + \varepsilon\left(T_3 - T_5\right) \tag{4}$$

where the heat exchanger effectiveness, ε, has been assumed equal to 0.875 based on the work of Gonçalves *et al.* (2009), who performed tests in an refrigerator identical to the one investigated here.

In the model of Hermes *et al.* (2009), the evaporating and condensing pressures are calculated based on previously specified degrees of refrigerant superheating and subcooling at the evaporator and condenser exits, respectively. Therefore, the working pressures are calculated directly from,

$$p_e = p_{sat}\left(T_5 - \Delta T_{sup}\right) \tag{5}$$

$$p_c = p_{sat}\left(T_3 + \Delta T_{sub}\right) \tag{6}$$

This procedure not only eliminates potential convergence issues associated with methods based on the calculation of the refrigerant charge, but also adjusts the capillary tube geometry and the refrigerant charge automatically in order to provide a desired degree of superheating and subcooling, which is convenient for optimization processes involving component-level modifications.

2.2 Refrigerated compartments

Figure 3 shows a diagram of the energy and fluid flows within the refrigerated compartments. The evaporator air mass flow rate, m_{fan}, is split into two air streams by a damper, so that part of the air is supplied to the frozen-food compartment and the remainder to the fresh-food compartment. Energy balances involving the evaporator, the frozen- and the fresh-food compartments yield,

$$r\left(Q_e - W_{fan}\right) = UA_{fz}\left(T_a - T_{fz}\right) + R_m^{-1}\left(T_{ff} - T_{fz}\right) \tag{7}$$

$$(1-r)\left(Q_e - W_{fan}\right) = UA_{ff}\left(T_a - T_{ff}\right) - R_m^{-1}\left(T_{ff} - T_{fz}\right) \tag{8}$$

where $r=m_{fz}/m_{ef}$ is the freezer air flow rate fraction, and UA_{fz} and UA_{ff} are the overall thermal conductances of the frozen- and fresh-food compartments, respectively. R_m is the mullion thermal resistance defined as,

$$R_m^{-1} = r(1-r)m_{fan}c_{pa} + UA_m \tag{9}$$

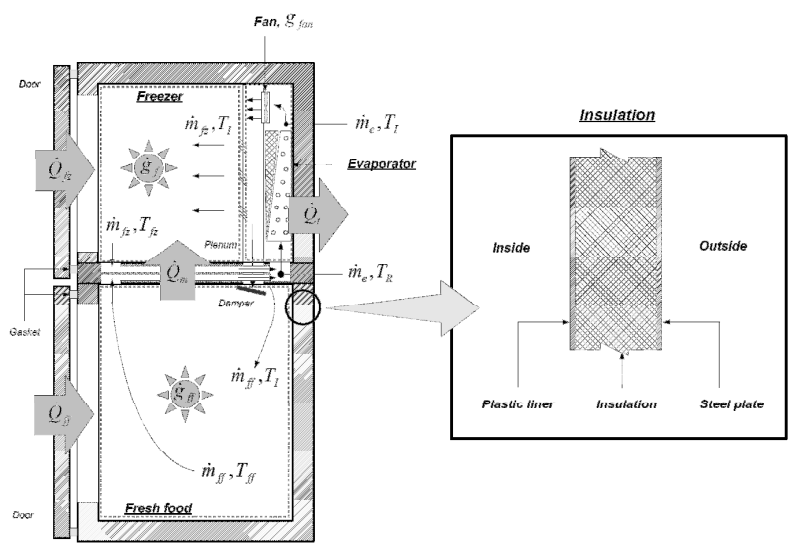

Figure 3. Mass and energy flows within the refrigerated compartments.

It is worth noting that the compartment temperatures are design constraints defined by test standards (AHAM: T_{ff}=7.2°C and T_{fz}=-15°C; ISO: T_{ff}=5°C and T_{fz}=-18°C). Therefore, Eqs. (7) to (9) must be solved for the air fraction, r, a parameter that balances the air flow between the frozen- and fresh-food compartments. Finally, the air temperature at the evaporator inlet and the supply air temperature are calculated from,

$$T_R = rT_{fz} + (1-r)T_{ff} \tag{10}$$

$$T_I = T_R - \left(Q_e - W_{fan}\right)/m_{fan}c_{pa} \tag{11}$$

The overall air-side pressure loss is given by,

$$\Delta p_{fan} = \Delta p_e + \Delta p_{cab} \tag{12}$$

where $\Delta p_{cab}=K_{ff}m_{ff}^2=K_{fz}m_{fz}^2$ is the pressure drop in both the frozen- and fresh-food compartments (see Fig. 3), and Δp_{fan} is the pressure head provided by the fan, which was correlated as follows (Waltrich, 2008),

$$\Delta p_{fan} = \sum_{i=0}^{3} e_i \, m_{fan}^i \tag{13}$$

The hydrodynamic coupling between the evaporator, the evaporator fan, and the refrigerated compartments is given by Eqs. (12) and (13), which are solved for the evaporator air flow rate. The fan curve coefficients, e_i, as well as the K_{fz} and K_{ff} factors, were obtained from a regression of experimental data (Waltrich, 2008).

The energy consumption is calculated assuming that the thermal load and the cooling capacity are nearly constant during the cycling regime. Therefore, the energy consumption can be estimated by an approximated runtime ratio calculated from the following energy balance over a running cycle,

$$\tau = \frac{t_{on}}{t_{on}+t_{off}} \cong \frac{UA_{ff}\left(T_a - T_{ff}\right) + UA_{fz}\left(T_a - T_{fz}\right) + W_{fan}}{Q_e} \tag{14}$$

Thus, the average energy consumption per time unit can be calculated from,

$$EC = \frac{1}{t_{on}+t_{off}} \int_0^{t_{on}+t_{off}} \left(\sum W\right) dt \cong \tau\left(W_k + W_{fan}\right) \tag{15}$$

and the system *COP* is given by,

$$COP = \frac{Q_e - W_{fan}}{W_k + W_{fan}} \cong \frac{UA_{ff}\left(T_a - T_{ff}\right) + UA_{fz}\left(T_a - T_{fz}\right)}{EC} \tag{16}$$

2.4 Numerical procedure and model validation

The model was implemented in the EES software (Klein, 2002). The input parameters are the working temperatures (T_a, T_{ff}, T_{fz}), the superheating and subcooling degrees and the compressor speed. Thus, for a given set of guessed values for p_e, p_c, h_1 and T_R, the compressor sub-model calculates h_2, the condenser sub-model estimates h_3 and $T_3=T(p_c,h_3)$, the internal heat exchanger sub-model calculates h_4 and T_1, and the evaporator sub-model calculates h_5 and $T_5=T(p_e,h_5)$. Finally, the cabinet thermal and hydraulic models are solved to estimate both r and τ. The calculation procedure is repeated until convergence is achieved.

The model results were compared with experimental data gathered in a refrigerator with 2 different evaporators at an ambient temperature of 32°C and compartment temperatures ranging from -28 to -17°C (frozen-food) and -11 to 9.2°C (fresh-food). The refrigerant charge was adjusted for each new configuration in order to keep both the subcooling and the superheating degrees between 2 and 3°C. Table 1 shows a comparison of the numerical results with the experimental data, where it can be observed that the model predicts the system *COP* to within ±5%, whereas the discrepancies between the calculated and measured compartment temperatures are between +1and -3°C.

3. OPTIMIZATION PROCEDURE

The optimization aims at finding the evaporator geometry that maximizes the thermal performance of the system according to a specific objective function. In the exercises conducted here, the following temperature constraints have been imposed: ambient at 32°C, frozen-food compartment at -18°C, fresh-food compartment at 5°C, and evaporator superheating and condenser subcooling of 1°C and 2°C, respectively. With respect to the evaporator geometry, the tube O.D. was fixed at 8.8 mm, the fin thickness at 0.25 mm, and the face area (height x width) at 59.5 x 307 mm^2. The following geometric parameters of the evaporator were changed during the optimization process: outlet height ($11.9 < H_2 < 59.45$ mm), number of fins ($30 < N_f < 60$), and evaporator length ($100 < L_t < 192$ mm). The evaporator geometry was generated automatically through the procedure illustrated in Fig. 4, where a uniform tube pitch of 21 mm (twice the radius of the tube bends) has been adopted (Waltrich, 2008).

Table 1. Comparison between model predictions and experimental data

Evaporator / Temperature set	Data	T_{fz} [°C]	T_{ff} [°C]	W_k [W]	p_e [bar]	p_c [bar]	*COP*
Original / Minimum	Calc.	-31.3	-12.5	93.3	0.60	10.9	1.06
	Meas.	-28.3	-10.4	104.7	0.65	11.6	1.05
	Diff.	-3.0°C	-2.1°C	-10.9%	-8.6%	-6.4%	1.4%
Original / Standard	Calc.	-20.0	4.4	127.1	0.86	12.4	1.21
	Meas.	-19.8	5.2	135.6	0.94	13.4	1.25
	Diff.	-0.2°C	-0.8°C	-6.3%	-9.1%	-7.0%	-3.4%
EFA / Minimum	Calc.	-30.0	-11.6	92.8	0.59	10.8	1.04
	Meas.	-27	-11.4	109.0	0.70	12.0	0.98
	Diff.	-3.0°C	-0.2°C	-14.9%	-15.4%	-9.8%	6.1%
EFA / Standard	Calc.	-19.1	3.6	123.0	0.83	12.2	1.17
	Meas.	-20.3	4.7	133.1	0.92	13.3	1.19
	Diff.	1.2°C	-1.1°C	-7.6%	-10.7%	-8.4%	-1.7%

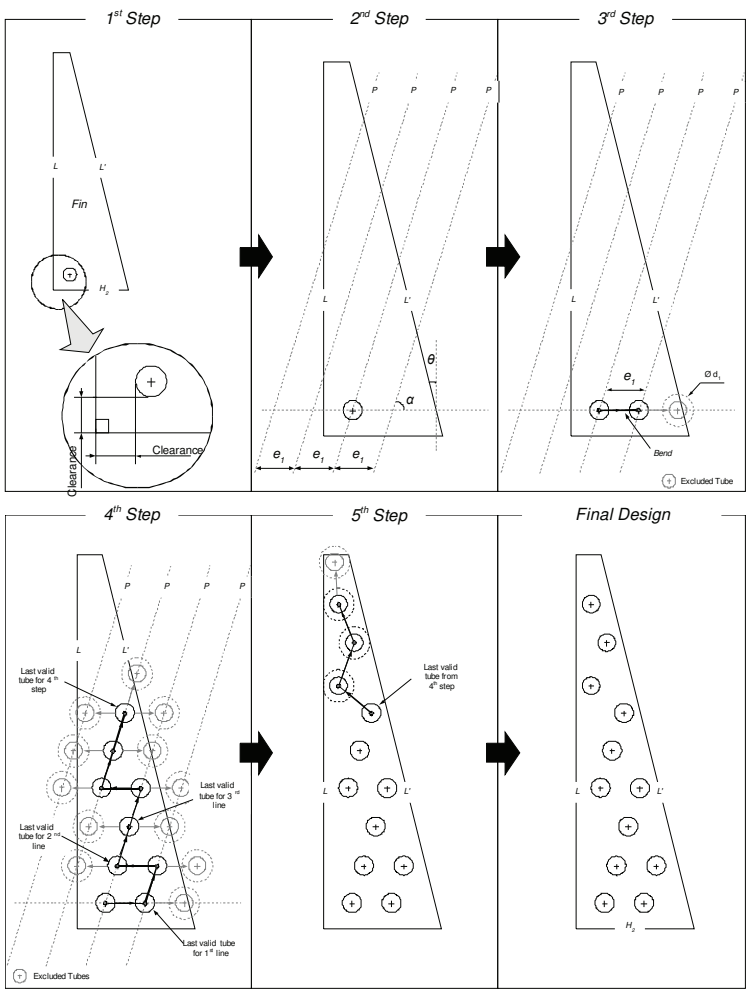

Figure 4. Automatic procedure for the AFE design.

To illustrate the procedure, two objective functions have been selected, the system *COP* and *PEC*=⟨*COP*⟩/⟨*M*⟩, where *M* is the mass of aluminum in the tube and fins, and ⟨ ⟩ is a normalization of a general variable Φ,

$$\langle \Phi \rangle = \frac{\Phi_{\#n} - \Phi_{min}}{\Phi_{max} - \Phi_{min}} + \frac{\Phi_{\#n}}{\Phi_{\#1}} \tag{17}$$

where the subscripts #1 and #*n* refer to the baseline and current configurations, respectively. The subscripts *max* and *min* refer to the maximum and minimum values of Φ for a given set of constraints that characterize the refrigeration system. The optimization was performed using the genetic algorithm routines of a commercial code (modeFRONTIER, 2005) linked to EES. Each run took approximately 4 hours in an Intel Core 2 1.8 GHz processor.

4. RESULTS

Figure 5 shows a parametric assessment of the *COP* and evaporator cost in terms of H_2 and L_t for a fixed number of fins (60). In Fig. 5.a, the system performance is seen to degenerate when H_2=H_1=59.5 mm. Moreover, the *COP* increases by 3% for H_2=43 mm with a cost reduction of 7%. Alternatively, a cost reduction of 40% can be achieved for H_2=22.5 mm, when the system *COP* decreases by only 1%. Figure 5.b shows that, for H_2=43.0 mm a small decrease in the evaporator length (to 0.170 m) yields a cost reduction of 25% without decreasing the system *COP*. By the same token, a 45% cost reduction can be achieved with a decrease in *COP* of only 1%.

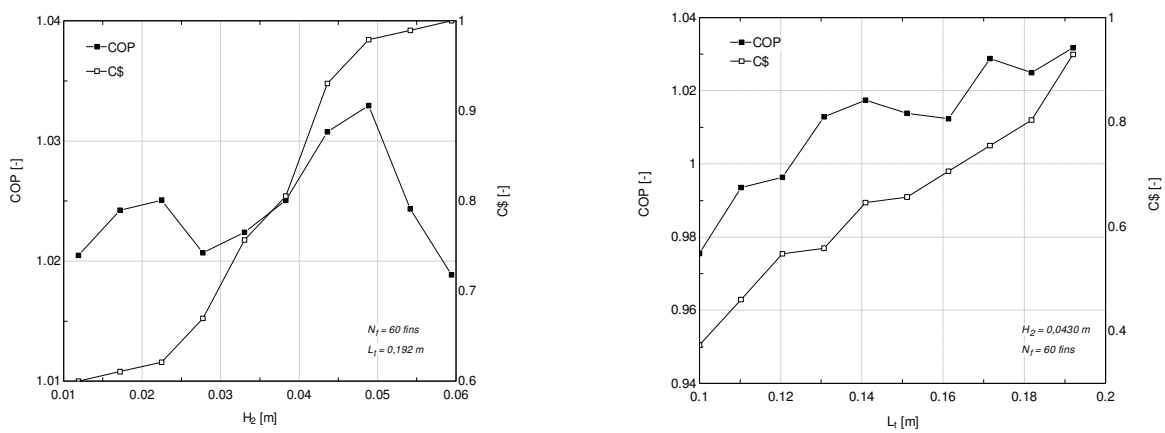

Figure 5. System *COP* and evaporator cost as a function of the (left) outlet height and (right) evaporator length.

Table 2 compares the best results obtained with both *COP* and *PEC*=⟨*COP*⟩/⟨*M*⟩, where it can be observed that the minimum energy consumption was achieved when the *COP* was the objective function. When the *PEC* is the objective function, the energy consumption increases with respect to the baseline and *COP*-based cases by 5.88 and 7.53%, respectively. Nevertheless, the amount of aluminum (and hence the cost of the evaporator) decreases by 71.1 and 69.6% with respect to the baseline and *COP*-based cases. It is noteworthy that in the *COP*-based case the number of fins decreases significantly. This result is beneficial in the sense that, for a larger number of fins, frost formation on the air-side can degrade the system performance (Knabben *et al.*, 2010). Thus, further advantage can be taken by optimizing the defrosting strategy.

5. CONCLUSIONS

A refrigerator simulation model comprised of sub-models for each component was used in a *COP*-based geometric optimization of the AFE. If, on the one hand, the *PEC* defined as the normalized ratio of the *COP* to the evaporator mass yielded a reduction of the evaporator cost by as much as 70% with a 7.8% decrease in the *COP*, on the other hand, when the system *COP* was the objective function, the *COP* increase by approximately 1%, whereas the amount of material decreased by 5.1% when compared to the baseline. A sensitivity analysis was also carried out showing that the system *COP* experienced only a modest variation with regard to the geometric parameters, ranging from 0.95 to 1.03 when the evaporator length was changed, and from 1.02 to 1.03 when the evaporator outlet height was varied.

Table 2. Summary of the optimization results.

Criterion	*Baseline*	*COP*	$\langle COP \rangle / \langle M \rangle$
H_2 [m]	0.0595	0.043	0.0245
N_f [fins]	60	60	39
L [m]	0.192	0.192	0.100
Δp_e [Pa]	0.9	2.0	1.4
Q_e [W]	122.0	125.9	97.3
W_{fan} [W]	5.8	5.7	5.7
W_k [W]	108.3	110.8	92.2
τ [-]	0.54	0.52	0.68
EC [kWh/day]	1.42	1.407	1.513
COP [-]	1.02	1.03	0.94
M [kg]	0.97	0.92	0.28
Geometry	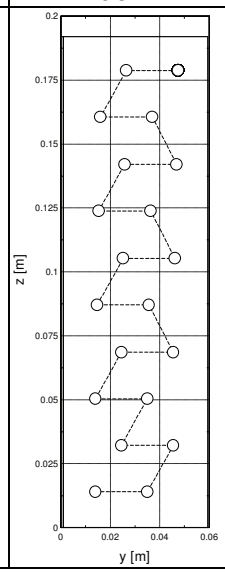	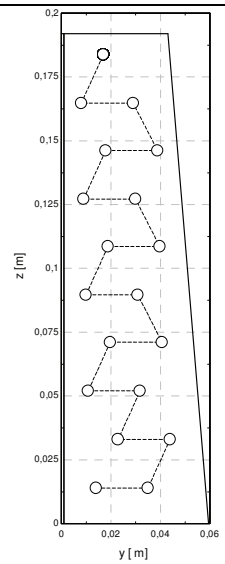	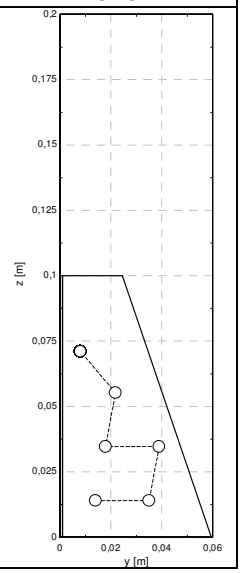

REFERENCES

Barbosa Jr. J.R., Melo C., Hermes C.J.L., Waltrich P., 2009, A Study of the Air-Side Heat Transfer and Pressure Drop Characteristics of Tube-Fin 'No-Frost' Evaporators, *Appl. Energy*, vol. 86: p. 1484-1491.

Cur N.O., Anselmino J.J., 1992, Evaporator for Home Refrigerator, US Patent 5,157,941.

Gonçalves J.M., Melo C., Hermes C.J.L., 2009, A semi-empirical model for steady-state simulation of household refrigerators, *Appl Thermal Eng.*, 29, pp.1622-1630

Hermes C.J.L., Melo C., Knabben F.T., Gonçalves J.M., 2009, Prediction of the energy consumption of household refrigerators and freezers via steady-state simulation, Applied Energy, 86, pp. 1311-1319.

Karatas, H., Dirik, E., Derbentil, T., 1996, An Experimental Study of Air-Side Heat Transfer and Friction Factor Correlations on Domestic Refrigerator Finned-Tube Evaporator Coils, 8th International Refrigeration and Air Conditioning Conference at Purdue, West Lafayette, IN, July 25-28.

Klein SA, 2002, EES – Engineering Equation Solver User's Manual, F-Chart Software, Middleton, WI.

Knabben, F.T., Hermes, C.J.L., Melo, C., 2010, Numerical Assessment of Frosting and Defrosting Processes in 'No-Frost' Evaporator Coils, Int. Refrig. and Air Cond. Conf. at Purdue, West Lafayette, IN, Paper 2111.

Lee, T.-H., Lee, J.-S., Oh, S.-Y., Lee, M.-Y., Lee, K.-S., 2002, Comparison of Air-Side Heat Transfer Coefficients of Several Types of Evaporators of Household Freezer/Refrigerators, 9th International Refrigeration and Air Conditioning Conference at Purdue, West Lafayette, IN, July 16-19.

Melo C., Hermes C.J.L., 2009, A heat transfer correlation for the natural draft wire-and-tube condensers, International Journal of Refrigeration, *Int. J. Refrig.*, vol. 32: p.546-555

Melo C., Piucco R.O., Duarte P.O.O., 2006, In-situ performance evaluation of 'no-frost' evaporators, 11th International Refrigeration and Air Conditioning Conference at Purdue, West Lafayette, IN, July 17-20, paper R076.

modeFRONTIER, 2005, Version 3.1.0, ESTECO.

Pira J.V., Bullard C.W., Jacobi A.M., 2000, An Evaluation of Heat Exchangers Using System Information and PEC, Air Conditioning and Refrigeration Center, ACRC Report TR-175, University of Illinois, Urbana, IL

Waltrich P.J., Barbosa Jr. J.R., Melo C., Hermes C.J.L., 2008, Air-side heat transfer and pressure drop in accelerated flow evaporators, 12th International Refrigeration and Air Conditioning Conference at Purdue, West Lafayette, IN, Paper 2311.

Waltrich, P.J., 2008, Analysis and optimization of accelerated flow evaporators for domestic refrigeration. M.Eng. thesis, Federal University of Santa Catarina, Florianopolis, SC, Brazil.

ACKNOWLEDGEMENTS

This study was carried out at the POLO facilities under National Grant No. 573581/2008-8 (National Institute of Science and Technology in Refrigeration and Thermophysics) funded by the CNPq Agency. Financial support from Whirlpool S.A. is also duly acknowledged.

NOMENCLATURE

A	area	(m^2)	**Subscripts**	
c_P	specific heat capacity	(J/kg.K)	a	air
H	evaporator height	(m)	c	condenser
h	heat transfer coefficient	($W/m^2.K$)	e	evaporator
K	pressure loss coefficient	(-)	f	fin
L	evaporator length	(m)	ff	fresh food
M	evaporator mass	(kg)	fz	freezer
$\dot{m}$	mass flow rate	(kg/s)	i	inlet
p	pressure	(Pa)	k	compressor
Q	heat transfer rate	(W)	o	outlet
R	flow resistance	($m^{-1}s^{-1}$)	R	return
T	temperature	(^oC)		
UA	overall thermal conductance	(W/K)		
V	velocity	(m/s)	**Greek symbols**	
v	specific volume	(m^3/kg)	τ	Runtime ratio
W	power	(W)	θ	AFE angle